Earth Syst. Dynam. Discuss., 2, 211–240, 2011
www.earth-syst-dynam-discuss.net/2/211/2011/
doi:10.5194/esdd-2-211-2011

Earth System Dynamics Discussions

Geologic constraints on earth system sensitivity to CO_2 during the Cretaceous and early Paleogene

D. L. Royer[1], M. Pagani[2], and D. J. Beerling[3]

[1]Department of Earth and Environmental Sciences and College of the Environment, Wesleyan University, Middletown, Connecticut, 06459, USA
[2]Department of Geology and Geophysics, Yale University, New Haven, Connecticut, 06520, USA
[3]Department of Animal and Plant Sciences, University of Sheffield, Sheffield, S10 2TN, UK

Received: 27 February 2011 – Accepted: 28 February 2011 – Published: 3 March 2011

Correspondence to: D. L. Royer (droyer@wesleyan.edu)

Published by Copernicus Publications on behalf of the European Geosciences Union.

Abstract

Earth system sensitivity (ESS) is the long-term (>10^3 yr) equilibrium temperature response to doubled CO_2. ESS has climate policy implications because global temperatures are not expected to decline appreciably for at least 10^3 yr, even if anthropogenic greenhouse-gas emissions drop to zero. We report quantitative ESS estimates of 3 °C or higher for much of the Cretaceous and early Paleogene based on paleo-reconstructions of CO_2 and temperature. These estimates are generally higher than climate sensitivities simulated from global climate models for the same ancient periods (∼3 °C). We conclude that climate models do not capture the full suite of positive climate feedbacks during greenhouse worlds. These absent feedbacks are probably related to clouds, trace greenhouse gases, seasonal snow cover, and/or vegetation, especially in polar regions. Continued warming in the coming decades as anthropogenic greenhouse gases accumulate in the atmosphere ensures that characterizing and quantifying these positive climate feedbacks will become a scientific challenge of increasing priority.

1 Introduction

Climate sensitivity is often defined as the change in global mean surface temperature for every doubling of atmospheric CO_2 (e.g., IPCC, 2007). In a simple blackbody system, forcing associated with CO_2 doubling (3.7 W m^{-2}) causes an ∼1.2 °C warming (Soden and Held, 2006). However, feedbacks such as changes in atmospheric water vapor content and cloud distributions amplify or dampen the temperature effect associated with CO_2. Climate sensitivity (CS) can therefore be defined as

$$\mathrm{CS} = \frac{1.2\,^{\circ}\mathrm{C}}{1 - f} \quad (1)$$

where f is the net impact of the feedback processes. In a landmark study based on global climate model (GCM) simulations, Charney (1979) calculated a climate sensitivity of $3 \pm 1.5\,^{\circ}$C, indicating a net amplifying effect for these feedbacks. This value, and its associated uncertainties (Roe and Baker, 2007; Knutti and Hegerl, 2008), has not substantially changed over the subsequent three decades of intense research using increasingly sophisticated climate models, historical records, and sedimentary archives back to the Last Glacial Maximum. For example, the IPCC (2007) reports a climate sensitivity of $3^{+1.5}_{-1.0}\,^{\circ}$C per CO_2 doubling.

1.1 Earth system sensitivity

The primary feedbacks considered by Charney (1979) and implemented in the majority of GCMs – changes in atmospheric water vapor content and cloud, snow, and sea ice distributions – all operate on short timescales ($<10^2$ yr). Some GCMs also include effects related to aerosols and vegetation (IPCC, 2007). For simplicity, we use the term Charney sensitivity to describe "fast-feedback" climate sensitivity associated with all of these models. Many of the climate feedbacks exluded from Charney sensitivity, such as the waxing and waning of continental ice sheets, impact climate primarily on longer timescales ($>10^2$ yr). Some "fast feedback" effects are excluded as well, especially those that are important only when the climate state is significantly different from today. For example, during globally-warm times characterized with little-to-no permanent ice, the behavior of clouds (Kump and Pollard, 2008) and the mixing ratios of other trace greenhouse gases (e.g., CH_4, N_2O) (Beerling et al., 2011) are not necessarily captured by the majority of GCMs. A calculation of climate sensitivity that integrates a whole-Earth system response to CO_2 change, including all slow- and fast-feedbacks, has been termed Earth system sensitivity (ESS) (Hansen et al., 2008; Lunt et al., 2010). ESS is a measure of the long-term equilibrium response to doubled CO_2 and can be formalized as

$$\mathrm{ESS} = \frac{1.2\,^{\circ}\mathrm{C}}{1 - (f_{\mathrm{C}} + f_{\mathrm{NC}})} \tag{2}$$

where f_C reflects Charney feedbacks and f_{NC} all other feedbacks.

ESS is more relevant than Charney sensitivity for understanding the ancient past because of the limits in temporal resolution of many geologic archives (often $>10^3$ yr) and because some climate feedbacks important in Earth's past are excluded from Charney sensitivity. ESS also has relevance for our current climate crisis by providing insights into the possible spectrum of long-term responses of the Earth system to anthropogenic atmospheric CO_2 increase. Although the full extent of future warming associated with ESS develops over centuries to millennia, it potentially contributes to significant temperature effects on shorter timescales too. For example, some processes absent in Charney sensitivity respond on decadal timescales, including ice sheet decay (Chen et al., 2006) and poleward migration of treelines (Sturm et al., 2001; Lloyd, 2005). Moreover, it is now recognized that global temperatures will not cool appreciably for many centuries, even if anthropogenic greenhouse-gas emissions drop to zero (Archer and Brovkin, 2008; Matthews and Caldeira, 2008; Shaffer et al., 2009; Solomon et al., 2009, 2010; Armour and Roe, 2011; Gillett et al., 2011). This is primarily because the transfer of heat and diffusion of CO_2 to the ocean are both linked to ocean circulation. Critically, these long-term temperature projections are based on climate models with a Charney-style climate sensitivity, even though their temporal scope overlaps with ESS. In this regard, estimations of ESS highlight the potential longer-term consequences of delaying policies for curbing greenhouse gas emissions (Archer, 2005; Montenegro et al., 2007).

1.2 Prior estimates of earth system sensitivity

The geologic record allows estimation of ESS because it captures feedbacks operating on short and very long timescales. Typically, ESS is computed from reconstructions of CO_2 and temperature (Table 1). The early Pliocene (5–3 million years ago, Ma) has received considerable attention in part because of the high density of paleoclimate information but also because it serves as a useful analog for the near future. At peak Pliocene warmth 4 to 5 Ma, global surface temperatures were ~4 °C warmer than pre-industrial conditions (Brierley and Fedorov, 2010). Coeval CO_2 estimates from a variety of approaches all indicate ~400 ppm, or ~0.5 CO_2 doublings relative to the pre-industrial (van der Burgh et al., 1993; Raymo et al., 1996; Pagani et al., 2010; Seki et al., 2010). After consideration of the uncertainties in the CO_2 and temperature estimates, a minimum ESS of 6 °C is implicated (Table 1) compared to a GCM-derived Charney sensitivity of 3 °C (Lunt et al., 2010). Paleoclimate analyses for the Pleistocene and Cenozoic glacial period (last 34 million years) also indicate an ~6 °C ESS (Hansen et al., 2008). The two-fold amplification of ESS over Charney sensitivity in this case is probably driven mostly by cryogenic feedbacks (Hansen et al., 2008; Pagani et al., 2010).

The apparent importance of cryogenic feedbacks raises the fundamental question of the nature of ESS during times in Earth's history lacking large ice sheets. The early Cretaceous to early Cenozoic (125–34 Ma) is key for addressing this question because it is the most recent and data-rich greenhouse interval (Table 1) (Frakes et al., 1992; Royer, 2006; Vaughan, 2007). Over the past ten years, many temperature reconstructions for this interval have warmed (Huber, 2008) while some CO_2 estimates have dropped (Breecker et al., 2010), implying an upward revision in ESS (Royer, 2010; Kiehl, 2011) and rendering earlier attempts at constraining ESS outdated (Budyko et al., 1987; Hoffert and Covey, 1992; Covey et al., 1996; Borzenkova, 2003) (Table 1).

ESS during the Paleocene-Eocene thermal maximum (PETM) ~55 Ma probably exceeded 4 °C (Higgins and Schrag, 2006; Pagani et al., 2006; Zeebe et al., 2009). This is an important observation because the PETM is considered a paleo-analog of present-day climate change in terms of rate and magnitude of carbon release (Zachos et al., 2008), albeit in an ice-free world. Bijl et al. (2010) produced a high-resolution CO_2 and temperature record for the Middle Eocene climatic optimum (MECO; 40 Ma) and calculated an ESS of 2–5 °C (Table 1). In a study encompassing most of the Phanerozoic,

Park and Royer (2011) optimized the value of ESS embedded in a long-term carbon cycle model to minimize the misfit in atmospheric CO_2 between the model and proxies. The most likely ESS values exceeded 3 °C during non-glacial intervals and ~6 °C during glacial periods (Table 1), although the time resolution was coarse (10 million year time-steps).

1.3 Goals of study

Elevated ESS relative to Charney sensitivity is observed for some glacial times but far less is known for non-glacial times outside of a few brief intervals (e.g., PETM, MECO). There is a clear need for better constraints on ESS during these warm times in order to evaluate the role of non-Charney feedbacks. Here we analyze early Cretaceous to early Paleogene (125–45 Ma) CO_2 and temperature records to establish new quantitative constraints on non-glacial ESS. Owing to the lack of strong cryogenic feedbacks during this period, we aim to assess whether ESS is similar to Charney sensitivity, and if there are differences to discuss the climate feedbacks that may be responsible.

2 Methods

We compiled temperature records for the 125–45 Ma interval from literature sources (Table 2). We use the Cramer et al. (2009) compilation of benthic foraminifera $\delta^{18}O$ values corrected for vital effects (Zachos et al., 2001) as a proxy for deep-water temperature. We also compiled tropical sea surface temperature (SST) data from three methods: $\delta^{18}O$ of planktonic foraminifera, Mg/Ca of planktonic foraminifera, and TEX_{86} of archaeal membrane lipids. All $\delta^{18}O$ records were chosen carefully to avoid diagenetically altered material (Pearson et al., 2001; Huber, 2008). TEX_{86} data are calibrated to Kim et al. (2008). Errors follow Crowley and Zachos (2000) for tropical $\delta^{18}O$ records (±2 °C), Kim et al. (2008) for TEX_{86} records (±1.7 °C), and the individual publications for Mg/Ca records.

We compiled proxy CO_2 records from the stomatal, phytoplankton, liverwort, and nahcolite methods (Table 2). All liverwort-based estimates are updated using the new atmospheric $\delta^{13}C$ record of Tipple et al. (2010). We exclude paleosol calcite- and goethite-based CO_2 estimates due to uncertainties in modeling soil respiration (Breecker et al., 2009) and isotopic fractionation factors (Rustad and Zarzycki, 2008), respectively. Boron-based CO_2 estimates of Pearson and Palmer (2000) are excluded due to problems related to diagenesis, vital effects of extinct species, and the evolution of seawater $\delta^{11}B$ and alkalinity (Lemarchand et al., 2000; Royer et al., 2001a; Pagani et al., 2005; Klochko et al., 2006, 2009).

Compiled atmospheric CO_2 and temperature records show considerable scatter at any given time slice (Fig. 1a–c); CO_2, for example, typically varies two-fold. Given these uncertainties, we conservatively calculate *minimum* values of ESS based on maximum estimates of atmospheric CO_2 and minimum estimates of global mean surface temperature. Our approach establishes the *minimum* level of long-term warming for any CO_2 change.

Calculation of earth system sensitivity

We calculate changes in global annual-mean surface temperature relative to pre-industrial conditions two independent ways following Hansen et al. (2008). First, tropical SSTs are converted to global mean surface temperature assuming a 2:3 scaling, consistent with Pleistocene records (Hansen et al., 2008), and a pre-industrial tropical SST of 29 °C (Fig. 1b). We note that our pre-industrial baseline is warm (compare with blue band in Fig. 1b) and that the 2:3 scaling is likely too conservative because latitudinal temperature gradients during the Cretaceous and early Paleogene were flatter than the present-day (Greenwood and Wing, 1995; Bice and Norris, 2002; Bijl et al., 2009; Hollis et al., 2009). A cooler SST baseline and a larger scaling factor both increase the calculation of global mean surface temperature and ESS. For example, during the Middle Eocene (~40 Ma), a period of flatter-than-present latitudinal temperature gradients (Bijl et al., 2009), Kiehl (2011) used tropical and subpolar SST records

(35–40 °C and 20–25 °C, respectively) to calculate a global temperature ~16 °C warmer than pre-industrial conditions. In contrast, our methodology returns a global temperature of 9.0–16.5 °C for the same tropical SST spread. This discrepancy reinforces our conservative approach in estimating ESS.

For benthic $\delta^{18}O$ temperature records, we assume no influence on $\delta^{18}O$ from ice and an ice-free ocean $\delta^{18}O$ of −1.2‰. We also assume a 1:1 scaling between high-latitude sourced deep-water and global temperatures for these non-glacial times. While changes in high-latitude surface-ocean temperature are generally amplified over the global surface ocean, the effect is compensated by amplified temperature change over land surfaces (Hansen et al., 2008). This 1:1 scaling, however, is not well constrained. To cast benthic-derived global surface temperatures relative to the pre-industrial, we note that deep-water temperatures just prior to the onset of Antarctic glaciation ~34 Ma were ~6 °C warmer than the pre-industrial (Zachos et al., 2008). Global surface temperature at this time was probably >6 °C warmer owing to the limit on deep-water temperatures by the freezing point during glacial periods. For example, a 2:3 scaling between deep-water and global temperatures is present during the Pleistocene (Hansen et al., 2008). In the spirit of establishing minimum changes in global surface temperature, we assume a conservative 1:1 scaling.

We determine the number of CO_2 doublings relative to pre-industrial time from the "max paleo-CO_2" line in Fig. 1a and a pre-industrial value of 280 ppm. CO_2 doublings are then converted to a projection of global mean surface temperature assuming a constant ESS value (colored lines in Fig. 1b–c). In this formulation, all actual temperature data plotting above a reference ESS line have an associated ESS that exceeds the reference value. We also compute ESS directly from the "max paleo-CO_2" history and individual temperature estimates (1 million year means shown in Fig. 1d). Because CO_2 was probably lower than our "max paleo-CO_2" reference, the ESS calculations are minima. However, CO_2 proxies, especially the stomatal proxy, lose precision at high CO_2 (see weakly-to-unbounded estimates in Fig. 1a) (Royer et al., 2001a; Beerling et al., 2009b).

Because the preceding analyses are normalized to pre-industrial conditions, it is necessary to consider additional effects of solar luminosity, continental position, and biological evolution, which impact temperature independently of CO_2. We account for the increase in solar luminosity over time (Gough, 1981) using a conversion factor of 0.8 °C W^{-1} (Hansen et al., 2005); at 125 Ma, for example, the correction for a reference line is 1.5 °C (note overall positive slope of reference lines in Fig. 1b–c). This correction is probably a minimum because it excludes the associated non-Charney feedback factors (f_{NC}).

Quantifying the impact of paleogeography on global temperatures is more uncertain. GCMs configured to the Cretaceous and early Paleogene, but with present-day luminosity, predict a warming of 0–2.8 °C relative to present-day control runs (Barron et al., 1993; Sloan and Rea, 1995; Heinemann et al., 2009; Dunkley Jones et al., 2010). However, these models exclude ice sheets, making direct comparisons to the present-day difficult, unless changing geography alone is sufficient to melt all ice sheets. Bice et al. (2000) varied only geography for a pair of simulations at 55 and 15 Ma (ice and greenhouse gas concentrations held constant) and found little difference in global temperature (<1 °C). Similarly, Donnadieu et al. (2006) performed simulations for the early and late Cretaceous and predicted a 3.8 °C warmer late Cretaceous. Changes in vegetation due to continental configuration can also impact climate. Vegetation models dynamically-coupled to climate models for the Cretaceous and Cenozoic predict a warming of ~2 °C over geographically-equivalent simulations with either no vegetation or a present-day vegetation distribution (Dutton and Barron, 1997; Otto-Bliesner and Upchurch, 1997). Because the paleovegetation schemes were prescribed based on fossil evidence, which in turn reflect a combination of geographic, evolutionary, and greenhouse-gas forcings, we consider 2 °C to represent a maximum temperature effect. In sum, the impact of geography, including linked vegetation feedback, is poorly constrained and as a result we exclude it from our calculations. If the effect is <3 °C, as seems likely from the preceding discussion, then our main conclusions remain unchanged.

3 Results

According to our new compilation of proxy data, atmospheric CO_2 declined from 600–1000 ppm at ~120 Ma to 300–700 ppm at 58 Ma, followed by a spike to near 2000 ppm at ~50 Ma (Fig. 1a). Both global temperature reconstructions follow the same pattern (Fig. 1b–c), highlighting a first-order link between CO_2 and temperature. Both benthic and tropical SST approaches to estimating ESS are broadly complementary, with most of the Cretaceous and early Paleogene record yielding ESS estimates of at least 3 °C (Fig. 1b–d). During the early Late Cretaceous (95–85 Ma), ESS might have exceeded 6 °C based on limited CO_2 data (Fig. 1d).

We consider a minimum ESS of 3 °C robust for several reasons. First, CO_2 appears internally consistent across methods, suggesting no strong methodological biases. However, a bias is present in the tropical SST data set, with TEX_{86} temperatures typically being the warmest, followed by Mg/Ca and then by $\delta^{18}O$ (Fig. 1b). The warm TEX_{86}-based temperatures may be related to calibration issues (Sluijs et al., 2011). Because of this methodological bias and because there are far fewer tropical data than benthic $\delta^{18}O$ data, we place more confidence in ESS estimates derived from deep-water temperature reconstructions (Fig. 1c).

Second, given the uncertainties in the CO_2 estimates (Fig. 1a), it could be argued that our "max paleo-CO_2" line is too low. However, even if CO_2 was consistently high (2000 ppm), ESS would still exceed 3 °C for much of the interval (dotted lines in Fig. 1b–c).

Third, because our results describe the mean ESS between the pre-industrial and a given geologic time slice, they could be biased by high ESS during glacial times (34–0 Ma). But even if glacial ESS was as high as 6 °C (Table 1), non-glacial ESS probably exceeded 3 °C (orange lines in Fig. 1b–c).

ESS is not static over time (Fig. 1d). This variability impacts our calculations because they are based on comparing an ancient time slice to pre-industrial conditions. Thus, the calculations are buffered in the sense that they are biased towards the mean

Discussion Paper | Discussion Paper | Discussion Paper | Discussion Paper |

ESS between tie-points. We note that this effect does not undermine our general conclusion of >3 °C ESS, but it is nonetheless informative to explore higher resolution patterns. One way forward is to use two ancient tie-points and avoid the pre-industrial altogether. While such a calculation also returns a mean ESS, the tie-points are more closely spaced. An additional benefit to this approach is that it circumvents many of the potential problems in calculating global mean surface temperature (see Methods) because one paleotemperature is subtracted from another. Also, the potential confounding effects of geography and biological evolution are minimized. A drawback, however, is that problems related to uncertainties in the paleoclimate reconstructions tend to be magnified two-fold. Thus, we consider the calculations provisional.

As noted earlier, the period from 58–50 Ma is marked by global warming (Fig. 1b–c). If we use the "max paleo-CO_2" trajectory and an overall 5.5 °C rise in global temperature (5.75 to 11.25 °C from benthic records; 2.0 to 7.5 °C from Mg/Ca tropical SST records), ESS during this interval is 3.7 °C. For the period 100–58 Ma, with a ΔT of −3.75 °C from benthic records, the corresponding ESS is 6.4 °C.

4 Discussion

Our analyses indicate that ESS was at least 3 °C for much of the Cretaceous and early Paleogene. We stress that this 3 °C value is not a mean "best-fit" estimate, but rather a likely minimum because most ESS estimates exceed 3 °C and because our methodology is designed to establish a minimum baseline. How do these minimum ESS estimates compare to Charney sensitivity? In the present-day climate system, IPCC (2007) considers <1.5 °C very unlikely (<10% probability) and the most likely range (with 66% confidence) between 2.0–4.5 °C (see also Fig. 2). However, a comparison to Charney sensitivity for the ancient past is more appropriate than for the present-day. Critically, GCMs for the Cretaceous and early Eocene simulate a mean Charney sensitivity of 2.0–2.8 °C (Barron et al., 1993; Sloan and Rea, 1995; Shellito

et al., 2003, 2009). If we collapse time in our individual ESS estimates (Fig. 1d), the resultant probability distribution indicates a mean of 4.9 °C (Fig. 2).

The totality of evidence suggests an ESS of at least 3 °C (Figs. 1b–d and 2) compared to a mean Charney sensitivity of 2.0–2.8 °C. We conclude from this that ESS was elevated relative to Charney sensitivity for at least some of the Cretaceous and early Paleogene. Positive climate feedbacks probably existed during these ice-free times that are either weak-to-absent today or that operate on timescales too slow to be captured by most GCMs. This model-data mismatch has profound consequences for understanding Earth system dynamics during these warm periods, for example the long-standing failure of GCMs in underestimating high-latitude temperatures and overestimating latitudinal temperature gradients (Barron et al., 1993; Wing and Greenwood, 1993; Greenwood and Wing, 1995; Valdes, 2000; Shellito et al., 2003, 2009; Schrag and Alley, 2004; Zachos et al., 2008; Bijl et al., 2009; Heinemann et al., 2009).

What feedbacks are responsible for high ESS during non-glacial times?

The identity of these "missing" feedbacks is uncertain. However, several biological feedbacks constitute "known unknowns", including other greenhouse gases (GHGs) and biogenic aerosols that could affect calculated ESS. Emissions of reactive biogenic gases from terrestrial ecosystems have substantial impacts on atmospheric chemistry (Arneth et al., 2010). In particular, they influence the tropospheric concentrations of GHGs such as ozone, methane, and nitrous oxide. Polar ice core records indicate that the biogeochemical processes controlling atmospheric CH_4 and N_2O concentrations are sensitive to climate change on glacial-interglacial (Spahni et al., 2005) and millennial timescales (Flückiger et al., 2004). However, climate feedbacks of these trace GHGs are missing from pre-Pleistocene climate modeling investigations that adopt fixed pre-industrial values regardless of the prescribed atmospheric CO_2 concentration.

Methane is a radiatively-important GHG and wetlands are the largest natural source of methane to the atmosphere. Sedimentary evidence indicates that methane-producing wetland environments were more extensive in the past, particularly in the early Eocene, with the potential steady-state flux sufficient to raise atmospheric concentrations to several thousand parts per billion (Beerling et al., 2009a). This, in turn, could also lead to higher stratospheric water vapor and polar stratospheric clouds (PSCs), due to oxidation, and result in surface warming, but the associated uncertainty here is high because the very large changes in PSCs are prescribed rather than evolved in a self-consistent manner from the models (Sloan et al., 1992; Kirk-Davidoff et al., 2002). Three-dimensional "earth system" modeling studies (latitude × longitude × height) characterizing ecosystem-chemistry climate interactions in the early Eocene (55 Ma) and late Cretaceous (90 Ma) greenhouse worlds independently indicate the clear potential for sustained elevated concentrations of methane (4–5 × pre-industrial levels) and other trace GHGs at these times (Beerling et al., 2011). Higher concentrations of trace GHGs exert a global planetary heating of 2 °C amplified by lower surface albedo feedbacks in the high latitudes to >6 °C (Beerling et al., 2011). Experimental work indicates elevated atmospheric CO_2 concentration can affect methane emissions from wetland systems (Megonigal and Schlesinger, 1997; Saarnio et al., 2000; Ellis et al., 2009). Hence, there should be feedback between atmospheric CO_2 and CH_4, which has strong relevance for understanding ESS. This expectation is supported by 3-D earth system simulations showing a similar CO_2 dependency of wetland CH_4 fluxes that increased ESS (2 × CO_2 to 4 × CO_2) by 1–4 °C during the late Cretaceous and early Eocene (Beerling et al., 2011).

Inclusion of ecosystem-atmospheric chemistry interactions into pre-Pleistocene GCMs highlights a further neglected biological feedback involving the effects of biogenic emissions of volatile organic compounds which can partition into the solid phase to form secondary organic aerosols (SOA) (Carslaw et al., 2010). Secondary organic aerosols affect the radiative balance of the atmosphere directly by scattering incoming solar radiation and indirectly through the formation cloud condensation nuclei (CCN) (Carslaw et al., 2010). The climate feedbacks of the ecosystem-aerosol interactions have yet to be investigated for the past or the present-day but could be important

contributory factors influencing ESS (Arneth et al., 2010). However, the atmospheric concentration of SOA is determined by emissions of volatile organic compounds from terrestrial ecosystems, and changes in temperature, humidity, precipitation, causing complex non-linear interactions under warmer or cooler climate regimes. Current understanding suggests increased SOA loading in the future may represent a negative climate feedback (Carslaw et al., 2010) that could decrease ESS to a CO_2 doubling.

In terms of marine biogenic aerosols, Kump and Pollard (2008) obtained dramatic results from prescribed reductions in marine aerosol production by phytoplankton in the Cretaceous. Assuming thermal stress in the Cretaceous oceans reduced dimethlysulfide production by phytoplankton, these idealized calculations led to a reduced abundance of CCN and less extensive cloud cover. Whether such assumptions are justified for past glacial and non-glacial climate states remains to be investigated. Nevertheless, as a result of decreased cloud cover reducing the reflection of incoming solar energy, polar temperatures rose dramatically by 10–15 °C (Kump and Pollard, 2008). Clearly, the properties of aerosols leading to cloud formation are an important and neglected aspect of global climate model assessment of ESS both for present-day and past climates. This issue is highlighted by recent work suggesting that cloud parameterization schemes in climate models may be tuned to a modern "dirty" atmosphere, giving an unrepresentatively high abundance of CCN compared to that expected in a pristine pre-industrial atmosphere (Kiehl, 2009). More appropriate constraints on CCN could therefore exert profound effects on climate simulations of continental interiors of past warm climate intervals (Kiehl, 2009). Unfortunately, our level of scientific understanding for all of these "known unknowns" is very low. This necessarily limits confidence in ESS estimates derived from the current generation of GCMs, and drawing conclusions by comparison with empirical datasets (Table 1).

5 Conclusions

A growing body of evidence supports an Earth-system climate sensitivity exceeding 6 °C during glacial times and at least 3 °C during non-glacial times. These estimates are likely higher than the abundant estimates of climate sensitivity that include only a subset of fast feedbacks (Charney climate sensitivity, ~3 °C). The feedbacks responsible for the disparity in a non-glaciated world are not well known because they are (presumably) weak-to-absent today and thus difficult to identify with Earth observation programs. Nonetheless, geological evidence and GCMs implicate clouds and other trace greenhouse gases as possible forcings. As these missing feedbacks are clarified, they can be incorporated into standard runs of paleo-GCMs. Doing so may help solve long-standing model-data mismatches, in particular the estimation by models of too-cool high latitudes. More robust GCMs will not only improve our understanding of climate dynamics in ancient greenhouse times, but improve future climate predictions as we move towards a new greenhouse world.

Acknowledgements. We thank Jerry Dickens for helpful comments on an earlier draft of the manuscript. D. L. R. thanks the Mellon Foundation for supporting a College of the Environment fellowship. M. P. acknowledges support from National Science Foundation and the Yale Climate and Energy Institute. D. J. B. gratefully acknowledges support through a Royal Society-Wolfson Research Merit Award.

References

Archer, D.: Fate of fossil fuel CO_2 in geologic time, J. Geophys. Res., 110, C09S05, doi:10.1029/2004JC002625, 2005.

Archer, D. and Brovkin, V.: The millennial atmospheric lifetime of anthropogenic CO_2, Climatic Change, 90, 283–297, 2008.

Armour, K. C. and Roe, G. H.: Climate commitment in an uncertain world, Geophys. Res. Lett., 38, L01707, doi:10.1029/2010GL045850, 2011.

Arneth, A., Harrison, S. P., Zaehle, S., Tsigaridis, K., Menon, S., Bartlein, P. J., and Feichter, J.: Terrestrial biogeochemical feedbacks in the climate system, Nat. Geosci., 3, 525–532, 2010.

Barron, E. J., Fawcett, P. J., Pollard, D., and Thompson, S.: Model simulations of Cretaceous climates: the role of geography and carbon dioxide, Philos. T. Roy. Soc. B, 341, 307–316, 1993.

Beerling, D. J., Lomax, B. H., Royer, D. L., Upchurch, G. R., and Kump, L. R.: An atmospheric pCO_2 reconstruction across the Cretaceous-Tertiary boundary from leaf megafossils, P. Natl. Acad. Sci. USA, 99, 7836–7840, 2002.

Beerling, D. J., Berner, R. A., Mackenzie, F. T., Harfoot, M. B., and Pyle, J. A.: Methane and the CH_4-related greenhouse effect over the past 400 million years, Am. J. Sci., 309, 97–113, 2009a.

Beerling, D. J., Fox, A., and Anderson, C. W.: Quantitative uncertainty analyses of ancient atmospheric CO_2 estimates from fossil leaves, Am. J. Sci., 309, 775–787, 2009b.

Beerling, D. J., Fox, A., Stevenson, D. S., and Valdes, P. J.: Enhanced chemistry-climate feedbacks in past greenhouse worlds, P. Natl. Acad. Sci. USA, in review, 2011.

Bice, K. L. and Norris, R. D.: Possible atmospheric CO_2 extremes of the Middle Cretaceous (late Albian-Turonian), Paleoceanography, 17(4), 1070, doi:10.1029/2002PA000778, 2002.

Bice, K. L., Scotese, C. R., Seidov, D., and Barron, E. J.: Quantifying the role of geographic change in Cenozoic ocean heat transport using uncoupled atmosphere and ocean models, Palaeogeogr. Palaeocl., 161, 295–310, 2000.

Bice, K. L., Birgel, D., Metyers, P. A., Dahl, K. A., Hinrichs, K.-U., and Norris, R. D.: A multiple proxy and model study of Cretaceous upper ocean temperatures and atmospheric CO_2 concentration, Paleoceanography, 21, PA2002, doi:10.1029/2005PA001203, 2006.

Bijl, P. K., Schouten, S., Sluijs, A., Reichart, G.-J., Zachos, J. C., and Brinkhuis, H.: Early Palaeogene temperature evolution of the southwest Pacific Ocean, Nature, 461, 776–779, 2009.

Bijl, P. K., Houben, A. J. P., Schouten, S., Bohaty, S. M., Sluijs, A., Reichart, G.-J., Sinninghe Damsté, J. S., and Brinkhuis, H.: Transient Middle Eocene atmospheric CO_2 and temperature variations, Science, 330, 819–821, 2010.

Bornemann, A., Norris, R. D., Friedrich, O., Beckmann, B., Schouten, S., Sinninghe Damsté, J. S., Vogel, J., Hofmann, P., and Wagner, T.: Isotopic evidence for glaciation during the Cretaceous supergreenhouse, Science, 319, 189–192, 2008.

Borzenkova, I. I.: Determination of global climate sensitivity to the gas composition of the atmosphere from paleoclimatic data, Izv. Atmos. Ocean. Phys., 39, 197–202, 2003.

Breecker, D. O., Sharp, Z. D., and McFadden, L. D.: Seasonal bias in the formation and stable isotopic composition of pedogenic carbonate in modern soils from central New Mexico, USA, Geol. Soc. Am. Bull., 121, 630–640, 2009.

Breecker, D. O., Sharp, Z. D., and McFadden, L. D.: Atmospheric CO_2 concentrations during ancient greenhouse climates were similar to those predicted for A.D. 2100, P. Natl. Acad. Sci. USA, 107, 576–580, 2010.

Brierley, C. M. and Fedorov, A. V.: Relative importance of meridional and zonal sea surface temperature gradients for the onset of the ice ages and Pliocene-Pleistocene climate evolution, Paleoceanography, 25, PA2214, doi:10.1029/2009PA001809, 2010.

Budyko, M. I., Ronov, A. B., and Yanshin, A. L.: History of the Earth's Atmosphere, Springer-Verlag, Berlin, 1987.

Carslaw, K. S., Boucher, O., Spracklen, D. V., Mann, G. W., Rae, J. G. L., Woodward, S., and Kulmala, M.: A review of natural aerosol interactions and feedbacks within the Earth system, Atmos. Chem. Phys., 10, 1701–1737, doi:10.5194/acp-10-1701-2010, 2010.

Charney, J.: Carbon dioxide and climate: a scientific assessment, National Academy of Sciences Press, Washington, DC, 1979.

Chen, J. L., Wilson, C. R., and Tapley, B. D.: Satellite gravity measurements confirm accelerated melting of Greenland ice sheet, Science, 313, 1958–1960, 2006.

Covey, C., Sloan, L. C., and Hoffert, M. I.: Paleoclimate data constraints on climate sensitivity: the paleocalibration method, Climatic Change, 32, 165–184, 1996.

Cramer, B. S., Toggweiler, J. R., Wright, J. D., Katz, M. E., and Miller, K. G.: Ocean overturning since the Late Cretaceous: inferences from a new benthic foraminiferal isotope compilation, Paleoceanography, 24, PA4216, doi:10.1029/2008PA001683, 2009.

Crowley, T. J., and Zachos, J. C.: Comparison of zonal temperature profiles for past warm time periods, in: Warm Climates in Earth History, edited by: Huber, B. T., MacLeod, K. G., and Wing, S. L., Cambridge University Press, Cambridge, 50–76, 2000.

DeConto, R. M. and Pollard, D.: Rapid Cenozoic glaciation of Antarctica induced by declining atmospheric CO_2, Nature, 421, 245–249, 2003.

DeConto, R. M., Pollard, D., Wilson, P. A., Pälike, H., Lear, C. H., and Pagani, M.: Thresholds for Cenozoic bipolar glaciation, Nature, 455, 652–656, 2008.

Donnadieu, Y., Pierrehumbert, R., Jacob, R., and Fluteau, F.: Modelling the primary control of paleogeography on Cretaceous climate, Earth Planet. Sc. Lett., 248, 426–437, 2006.

Dumitrescu, M., Brassell, S. C., Schouten, S., Hopmans, E. C., and Sinninghe Damsté, J. S.: Instability in tropical Pacific sea-surface temperatures during the early Aptian, Geology, 34, 833–836, 2006.

Dunkley Jones, T., Ridgwell, A., Lunt, D. J., Maslin, M. A., Schmidt, D. N., and Valdes, P. J.: A Paleogene perspective on climate sensitivity and methane hydrate instability, Philos. T. Roy. Soc. A, 368, 2395–2415, 2010.

Dutton, J. E. and Barron, E. J.: Miocene to present vegetation changes: A possible piece of the Cenozoic cooling puzzle, Geology, 25, 39–41, 1997.

Ellis, T., Hill, P. W., Fenner, N., Williams, G. G., Godbold, D., and Freeman, C.: The interactive effects of elevated carbon dioxide and water table draw-down on carbon cycling in a Welsh ombrotrophic bog, Ecol. Eng., 35, 978–986, 2009.

Fletcher, B. J., Brentnall, S. J., Anderson, C. W., Berner, R. A., and Beerling, D. J.: Atmospheric carbon dioxide linked with Mesozoic and early Cenozoic climate change, Nat. Geosci., 1, 43–48, 2008.

Flückiger, J., Blunier, T., Stauffer, B., Chappellaz, J., Spahni, R., Kawamura, K., Schwander, J., Stocker, T. F., and Dahl-Jensen, D.: N_2O and CH_4 variations during the last glacial epoch: Insight into global processes, Global Biogeochem. Cy., 18, GB1020, doi:10.1029/2003GB002122, 2004.

Forster, A., Schouten, S., Baas, M., and Sinninghe Damsté, J. S.: Mid-Cretaceous (Albian Santonian) sea surface temperature record of the tropical Atlantic Ocean, Geology, 35, 919–922, 2007a.

Forster, A., Schouten, S., Moriya, K., Wilson, P. A., and Sinninghe Damsté, J. S.: Tropical warming and intermittent cooling during the Cenomanian/Turonian oceanic anoxic event 2: sea surface temperature records from the equatorial Atlantic, Paleoceanography, 22, PA1219, doi:10.1029/2006PA001349, 2007b.

Frakes, L. A., Francis, J. E., and Syktus, J. I.: Climate Modes of the Phanerozoic, Cambridge University Press, Cambridge, 274 pp., 1992.

Freeman, K. H. and Hayes, J. M.: Fractionation of carbon isotopes by phytoplankton and estimates of ancient CO_2 levels, Global Biogeochem. Cy., 6, 185–198, 1992.

Gillett, N. P., Arora, V. K., Zickfeld, K., Marshall, S. J., and Merryfield, W. J.: Ongoing climate change following a complete cessation of carbon dioxide emissions, Nat. Geosci., 4, 83–87, 2011.

Gough, D. O.: Solar interior structure and luminosity variations, Sol. Phys., 74, 21–34, 1981.

Greenwood, D. R. and Wing, S. L.: Eocene continental climates and latitudinal temperature gradients, Geology, 23, 1044–1048, 1995.

Greenwood, D. R., Scarr, M. J., and Christophel, D. C.: Leaf stomatal frequency in the Australian tropical rainforest tree *Neolitsea dealbata* (Lauraceae) as a proxy measure of atmospheric $p\mathrm{CO}_2$, Palaeogeogr. Palaeocl., 196, 375–393, 2003.

Hansen, J., Sato, M., Ruedy, R., Nazarenko, L., Lacis, A., Schmidt, G. A., Russell, G., Aleinov, I., Bauer, M., Bauer, S., Bell, N., Cairns, B., Canuto, V., Chandler, M., Cheng, Y., Genio, A. D., Faluvegi, G., Fleming, E., Friend, A., Hall, T., Jackman, C., Kelley, M., Kiang, N., Koch, D., Lean, J., Lerner, J., Lo, K., Menon, S., Miller, R., Minnis, P., Novakov, T., Oinas, V., Perlwitz, J., Perlwitz, J., Rind, D., Romanou, A., Shindell, D., Stone, P., Sun, S., Tausnev, N., Thresher, D., Wielicki, B., Wong, T., Yao, M., and Zhang, S.: Efficacy of climate forcings, J. Geophys. Res., 110, D18104, doi:10.1029/2005JD005776, 2005.

Hansen, J., Sato, M., Kharecha, P., Beerling, D., Berner, R., Masson-Delmotte, V., Pagani, M., Raymo, M., Royer, D. L., and Zachos, J. C.: Target atmospheric CO_2: where should humanity aim?, Open Atmos. Sci. J., 2, 217–231, 2008.

Haworth, M., Hesselbo, S. P., McElwain, J. C., Robinson, S. A., and Brunt, J. W.: Mid-Cretaceous $p\mathrm{CO}_2$ based on stomata of the extinct conifer *Pseudofrenelopsis* (Cheirolepidiaceae), Geology, 33, 749–752, 2005.

Hegerl, G. C., Crowley, T. J., Hyde, W. T., and Frame, D. J.: Climate sensitivity constrained by temperature reconstructions over the past seven centuries, Nature, 440, 1029–1032, 2006.

Heinemann, M., Jungclaus, J. H., and Marotzke, J.: Warm Paleocene/Eocene climate as simulated in ECHAM5/MPI-OM, Clim. Past, 5, 785–802, doi:10.5194/cp-5-785-2009, 2009.

Higgins, J. A. and Schrag, D. P.: Beyond methane: Towards a theory for the Paleocene-Eocene Thermal Maximum, Earth Planet. Sc. Lett., 245, 523–537, 2006.

Hoffert, M. I. and Covey, C.: Deriving global climate sensitivity from palaeoclimate reconstructions, Nature, 360, 573–576, 1992.

Hollis, C. J., Handley, L., Crouch, E. M., Morgans, H. E. G., Baker, J. A., Creech, J., Collins, K. S., Gibbs, S. J., Huber, M., Schouten, S., Zachos, J. C., and Pancost, R. D.: Tropical sea temperatures in the high-latitude South Pacific during the Eocene, Geology, 37, 99–102, 2009.

Huber, M.: A hotter greenhouse?, Science, 321, 353–354, 2008.

Jagniecki, E., Lowenstein, T. K., and Jenkins, D.: Sodium carbonates: temperature and $p\mathrm{CO}_2$ indicators for ancient and modern alkaline saline lakes, Geol. Soc. Am. Abstracts with Programs, Paper No. 165-402, 42(5), 404, 2010.

Kiehl, J. T.: Challenges in modeling warm Cenozoic climates, Geochim. Cosmochim. Acta, 73(S1), A648, 2009.

Kiehl, J. T.: Lessons from Earth's past, Science, 331, 158–159, 2011.

Kim, J.-H., Schouten, S., Hopmans, E. C., Donner, B., and Sinninghe Damsté, J. S.: Global sediment core-top calibration of the TEX_{86} paleothermometer in the ocean, Geochim. Cosmochim. Acta, 72, 1154–1173, 2008.

Kirk-Davidoff, D. B., Schrag, D. P., and Anderson, J. G.: On the feedback of statospheric clouds and polar climate, Geophys. Res. Lett., 29, 1556, doi:10.1029/2002GL014659, 2002.

Klochko, K., Kaufman, A. J., Yao, W. S., Byrne, R. H., and Tossell, J. A.: Experimental measurement of boron isotope fractionation in seawater, Earth Planet. Sc. Lett., 248, 276–285, 2006.

Klochko, K., Cody, G. D., Tossell, J. A., Dera, P., and Kaufman, A. J.: Re-evaluating boron speciation in biogenic calcite and aragonite using ^{11}B MAS NMR, Geochim. Cosmochim. Acta, 73, 1890–1900, 2009.

Knutti, R. and Hegerl, G. C.: The equilibrium sensitivity of the Earth's temperature to radiation changes, Nat. Geosci., 1, 735–743, 2008.

Kürschner, W. M., Wagner, F., Dilcher, D. L., and Visscher, H.: Using fossil leaves for the reconstruction of Cenozoic paleoatmospheric CO_2 concentrations, in: Geological Perspectives of Global Climate Change, edited by: Gerhard, L. C., Harrison, W. E., and Hanson, B. M., The American Association of Petroleum Geologists, Tulsa, 169–189, 2001.

Kump, L. R. and Pollard, D.: Amplification of Cretaceous warmth by biological cloud feedbacks, Science, 320, 195, 2008.

Lemarchand, D., Gaillardet, J., Lewin, É., and Allègre, C. J.: The influence of rivers on marine boron isotopes and implications for reconstructing past ocean pH, Nature, 408, 951–954, 2000.

Lloyd, A. H.: Ecological histories from Alaskan tree lines provide insight into future change, Ecology, 86, 1687–1695, 2005.

Lowenstein, T. K. and Demicco, R. V.: Elevated Eocene atmospheric CO_2 and its subsequent decline, Science, 313, 1928, 2006.

Lunt, D. J., Haywood, A. M., Schmidt, G. A., Salzmann, U., Valdes, P. J., and Dowsett, H. J.: Earth system sensitivity inferred from Pliocene modelling and data, Nat. Geosci., 3, 60–64, 2010.

Matthews, H. D. and Caldeira, K.: Stabilizing climate requires near-zero emissions, Geophys. Res. Lett., 35, L04705, doi:10.1029/2007GL032388, 2008.

Megonigal, J. P. and Schlesinger, W. H.: Enhanced CH_4 emission from a wetland soil exposed to elevated CO_2, Biogeochemistry, 37, 77–88, 1997.

Montenegro, A., Brovkin, V., Eby, M., Archer, D., and Weaver, A. J.: Long term fate of anthropogenic carbon, Geophys. Res. Lett., 34, L19707, doi:10.1029/2007GL030905, 2007.

Moriya, K., Wilson, P. A., Friedrich, O., Erbacher, J., and Kawahata, H.: Testing for ice sheets during the mid-Cretaceous greenhouse using glassy foraminiferal calcite from the mid-Cenomanian tropics on Demerara Rise, Geology, 35, 615–618, 2007.

Norris, R. D., Bice, K. L., Magno, E. A., and Wilson, P. A.: Jiggling the tropical thermostat in the Cretaceous hothouse, Geology, 30, 299–302, 2002.

Otto-Bliesner, B. L. and Upchurch, G. R.: Vegetation-induced warming of high-latitude regions during the Late Cretaceous period, Nature, 385, 804–807, 1997.

Pagani, M., Lemarchand, D., Spivack, A., and Gaillardet, J.: A critical evaluation of the boron isotope-*p*H proxy: The accuracy of ancient ocean *p*H estimates, Geochim. Cosmochim. Acta, 69, 953–961, 2005.

Pagani, M., Caldeira, K., Archer, D., and Zachos, J. C.: An ancient carbon mystery, Science, 314, 1556–1557, 2006.

Pagani, M., Liu, Z., LaRiviere, J., and Ravelo, A. C.: High Earth-system climate sensitivity determined from Pliocene carbon dioxide concentrations, Nat. Geosci., 3, 27–30, 2010.

Park, J. and Royer, D. L.: Geologic constraints on the glacial amplification of Phanerozoic climate sensitivity, Am. J. Sci., in press, 2011.

Passalia, M. G.: Cretaceous pCO_2 estimation from stomatal frequency analysis of gymnosperm leaves of Patagonia, Argentina, Palaeogeogr. Palaeocl., 273, 17–24, 2009.

Pearson, P. N. and Palmer, M. R.: Atmospheric carbon dioxide concentrations over the past 60 million years, Nature, 406, 695–699, 2000.

Pearson, P. N., Ditchfield, P. W., Singano, J., Harcourt-Brown, K. G., Nicholas, C. J., Olsson, R. K., Shackleton, N. J., and Hall, M. A.: Warm tropical sea surface temperatures in the Late Cretaceous and Eocene epochs, Nature, 413, 481–487, 2001.

Pearson, P. N., van Dongen, B. E., Nicholas, C. J., Pancost, R. D., Schouten, S., Singano, J. M., and Wade, B. S.: Stable warm tropical climate through the Eocene Epoch, Geology, 35, 211–214, 2007.

Pearson, P. N., Foster, G. L., and Wade, B. S.: Atmospheric carbon dioxide through the Eocene-Oligocene climate transition, Nature, 461, 1110–1113, 2009.

Pollard, D. and DeConto, R. M.: Hysteresis in Cenozoic Antarctic ice-sheet variations, Global Planet. Change, 45, 9–21, 2005.

Pucéat, E., Lécuyer, C., Donnadieu, Y., Naveau, P., Cappetta, H., Ramstein, G., Huber, B. T., and Kriwet, J.: Fish tooth $\delta^{18}O$ revising Late Cretaceous meridional upper ocean water temperature gradients, Geology, 35, 107–110, 2007.

Quan, C., Sun, G., and Zhou, Z.: A new Tertiary *Ginkgo* (Ginkgoaceae) from the Wuyun Formation of Jiayin, Heilongjiang, northeastern China and its paleoenvironmental implications, Am. J. Bot., 97, 446–457, 2010.

Raymo, M. E., Grant, B., Horowitz, M., and Rau, G. H.: Mid-Pliocene warmth: stronger greenhouse and stronger conveyor, Mar. Micropaleontol., 27, 313–326, 1996.

Retallack, G. J.: Greenhouse crises of the past 300 million years, Geol. Soc. Am. Bull., 121, 1441–1455, 2009.

Roe, G. H. and Baker, M. B.: Why is climate sensitivity so unpredictable?, Science, 318, 629–632, 2007.

Royer, D. L.: Estimating latest Cretaceous and Tertiary atmospheric CO_2 concentration from stomatal indices, in: Causes and Consequences of Globally Warm Climates in the Early Paleogene, edited by: Wing, S. L., Gingerich, P. D., Schmitz, B., and Thomas, E., Geological Society of America Special Paper 369, Boulder, 79–93, 2003.

Royer, D. L.: CO_2-forced climate thresholds during the Phanerozoic, Geochim. Cosmochim. Acta, 70, 5665–5675, 2006.

Royer, D. L.: Fossil soils constrain ancient climate sensitivity, P. Natl. Acad. Sci. USA, 107, 517–518, 2010.

Royer, D. L., Berner, R. A., and Beerling, D. J.: Phanerozoic CO_2 change: evaluating geochemical and paleobiological approaches, Earth-Sci. Rev., 54, 349–392, 2001a.

Royer, D. L., Wing, S. L., Beerling, D. J., Jolley, D. W., Koch, P. L., Hickey, L. J., and Berner, R. A.: Paleobotanical evidence for near present-day levels of atmospheric CO_2 during part of the Tertiary, Science, 292, 2310–2313, 2001b.

Royer, D. L., Berner, R. A., and Park, J.: Climate sensitivity constrained by CO_2 concentrations over the past 420 million years, Nature, 446, 530–532, 2007.

Rustad, J. R. and Zarzycki, P.: Calculation of site-specific carbon-isotope fractionation in pedogenic oxide minerals, P. Natl. Acad. Sci. USA, 105, 10297–10301, 2008.

Saarnio, S., Saarinen, T., Vasander, H., and Silvola, J.: A moderate increase in the annual CH_4 efflux by raised CO_2 or NH_4NO_3 supply in a boreal oligotrophic mire, Global Change Biol., 6, 137–144, 2000.

Schouten, S., Hopmans, E. C., Forster, A., van Breugel, Y., Kuypers, M. M. M., and Sinninghe Damsté, J. S.: Extremely high sea-surface temperatures at low latitudes during the middle Cretaceous as revealed by archaeal membrane lipids, Geology, 31, 1069–1072, 2003.

Schrag, D. P. and Alley, R. B.: Ancient lessons for our future climate, Science, 306, 821–822, 2004.

Seki, O., Foster, G. L., Schmidt, D. N., Mackensen, A., Kawamura, K., and Pancost, R. D.: Alkenone and boron-based Pliocene pCO_2 records, Earth Planet. Sc. Lett., 292, 201–211, 2010.

Sexton, P. F., Wilson, P. A., and Pearson, P. N.: Microstructural and geochemical perspectives on planktic foraminiferal preservation: “glassy” versus “frosty”, Geochem. Geophy. Geosy., 7, Q12P19, doi:10.1029/2006GC001291, 2006.

Shaffer, G., Olsen, S. M., and Pedersen, J. O. P.: Long-term ocean oxygen depletion in response to carbon dioxide emissions from fossil fuels, Nat. Geosci., 2, 105–109, 2009.

Shellito, C. J., Sloan, L. C., and Huber, M.: Climate model sensitivity to atmospheric CO_2 levels in the Early-Middle Paleogene, Palaeogeogr. Palaeocl., 193, 113–123, 2003.

Shellito, C. J., Lamarque, J.-F., and Sloan, L. C.: Early Eocene Arctic climate sensitivity to pCO_2 and basin geography, Geophys. Res. Lett., 36, L09707, doi:10.1029/2009GL037248, 2009.

Silverman, B. W.: Density Estimation for Statistics and Data Analysis, Chapman & Hall, London, 1986.

Sloan, L. C. and Rea, D. K.: Atmospheric carbon dioxide and early Eocene climate: A general circulation modeling sensitivity study, Palaeogeogr. Palaeocl., 119, 275–292, 1995.

Sloan, L. C., Walker, J. C. G., Moore, T. C., Rea, D. K., and Zachos, J. C.: Possible methane-induced polar warming in the early Eocene, Nature, 357, 320–322, 1992.

Sluijs, A., Bijl, P. K., Schouten, S., Röhl, U., Reichart, G.-J., and Brinkhuis, H.: Southern ocean warming, sea level and hydrological change during the Paleocene-Eocene thermal maximum, Clim. Past, 7, 47–61, doi:10.5194/cp-7-47-2011, 2011.

Smith, R. Y., Greenwood, D. R., and Basinger, J. F.: Estimating paleoatmospheric pCO_2 during the Early Eocene Climatic Optimum from stomatal frequency of *Ginkgo*, Okanagan Highlands, British Columbia, Canada, Palaeogeogr. Palaeocl., 293, 120–131, 2010.

Soden, B. J. and Held, I. M.: An assessment of climate feedbacks in coupled ocean-atmosphere models, J. Climate, 19, 3354–3360, 2006.

Solomon, S., Plattner, G.-K., Knutti, R., and Friedlingstein, P.: Irreversible climate change due to carbon dioxide emissions, P. Natl. Acad. Sci. USA, 106, 1704–1709, 2009.

Solomon, S., Daniel, J. S., Sanford, T. J., Murphy, D. M., Plattner, G.-K., Knutti, R., and Friedlingstein, P.: Persistence of climate changes due to a range of greenhouse gases, P. Natl. Acad. Sci. USA, 107, 18354–18359, 2010.

Spahni, R., Chappellaz, J., Stocker, T. F., Loulergue, L., Hausammann, G., Kawamura, K., Flückiger, J., Schwander, J., Raynaud, D., Masson-Delmotte, V., and Jouzel, J.: Atmospheric methane and nitrous oxide of the Late Pleistocene from Antarctic ice cores, Science, 310, 1317–1321, 2005.

Sturm, M., Racine, C., and Tape, K.: Increasing shrub abundance in the Arctic, Nature, 411, 546–547, 2001.

Tipple, B. J., Meyers, S. R., and Pagani, M.: Carbon isotope ratio of Cenozoic CO_2: a comparative evaluation of available geochemical proxies, Paleoceanography, 25, PA3202, doi:10.1029/2009PA001851, 2010.

Tripati, A., Delaney, M. L., Zachos, J. C., Anderson, L. D., Kelly, D. C., and Elderfield, H.: Tropical sea-surface temperature reconstruction for the early Paleogene using Mg/Ca ratios of planktonic foraminifera, Paleoceanography, 18(4), 1101, doi:10.1029/2003PA000937, 2003.

Valdes, P. J.: Warm climate forcing mechanisms, in: Warm Climates in Earth History, edited by: Huber, B. T., MacLeod, K. G., and Wing, S. L., Cambridge University Press, Cambridge, 3–20, 2000.

van der Burgh, J., Visscher, H., Dilcher, D. L., and Kürschner, W. M.: Paleoatmospheric signatures in Neogene fossil leaves, Science, 260, 1788–1790, 1993.

Vaughan, A. P. M.: Climate and geology – a Phanerozoic perspective, in: Deep-Time Perspectives on Climate Change: Marrying the Signal from Computer Models and Biological Proxies, edited by: Williams, M., Haywood, A. M., Gregory, F. J., and Schmidt, D. N., The Geological Society and The Micropalaeontological Society, Special Publications, London, 5–59, 2007.

Wagner, T., Herrle, J. O., Sinninghe Damsté, J. S., Schouten, S., Stüsser, I., and Hofmann, P.: Rapid warming and salinity changes of Cretaceous surface waters in the subtropical North Atlantic, Geology, 36, 203–206, 2008.

Wilson, P. A. and Norris, R. D.: Warm tropical ocean surface and global anoxia during the mid-Cretaceous period, Nature, 412, 425–429, 2001.

Wilson, P. A. and Opdyke, B. N.: Equatorial sea-surface temperatures for the Maastrichtian revealed through remarkable preservation of metastable carbonate, Geology, 24, 555–558, 1996.

Wilson, P. A., Norris, R. D., and Cooper, M. J.: Testing the Cretaceous greenhouse hypothesis using glassy foraminiferal calcite from the core of the Turonian tropics on Demerara Rise, Geology, 30, 607–610, 2002.

Wing, S. L. and Greenwood, D. R.: Fossils and fossil climate: the case for equable continental interiors in the Eocene, Philos. T. Roy. Soc. B, 341, 243–252, 1993.

Zachos, J., Pagani, M., Sloan, L., Thomas, E., and Billups, K.: Trends, rhythms, and aberrations in global climate 65 Ma to present, Science, 292, 686–693, 2001.

Zachos, J. C., Dickens, G. R., and Zeebe, R. E.: An early Cenozoic perspective on greenhouse warming and carbon-cycle dynamics, Nature, 451, 279–283, 2008.

Zeebe, R. E., Zachos, J. C., and Dickens, G. R.: Carbon dioxide forcing alone insufficient to explain Palaeocene-Eocene Thermal Maximum warming, Nat. Geosci., 2, 576–580, 2009.

Table 1. Published estimates of Earth system sensitivity (ESS). All values are approximate. PETM = Paleocene-Eocene thermal maximum; MECO = Middle Eocene climatic optimum. Ma = million years ago. Park and Royer (2011) updates Royer et al. (2007).

Time period	ESS (°C)	Reference
Large ice sheets present		
Pleistocene (last 400 000 yr)	6	Hansen et al. (2008)
Pliocene (5–3 Ma)	>7	Pagani et al. (2010)
Pliocene (5–3 Ma)	6[a]	Budyko et al. (1987); Borzenkova (2003)
Cenozoic glacial (34–0 Ma)	6	Hansen et al. (2008)
Phanerozoic glacial (340–260, 40–0 Ma)	>6	Park and Royer (2011)
Large ice sheets absent		
Late Eocene (35 Ma)	High	Kiehl (2011)
MECO (40 Ma)	2–5	Bijl et al. (2010)
Early Eocene (55 Ma)	2.4[a,b]	Covey et al. (1996)
PETM (55.5 Ma)	4	Higgins and Schrag (2006)
PETM (55.5 Ma)	High	Pagani et al. (2006)
PETM (55.5 Ma)	High	Zeebe et al. (2009)
Cretaceous (100 Ma)	3.4[a,b]	Hoffert and Covey (1992)
Cretaceous-early Paleogene (110–45 Ma)	3.7[a]	Budyko et al. (1987); Borzenkova (2003)
Phanerozoic non-glacial (420–340, 260–40 Ma)	>3	Park and Royer (2011)

[a] Recalculated treating changes in albedo as part of the response.

[b] Recalculated assuming 3.7 $W\,m^{-2}$ for the radiative forcing of doubled CO_2 (IPCC, 2007).

Table 2. CO_2 and temperature records used in study.

Climate record	References
CO_2-stomata	Kürschner et al. (2001); Royer et al. (2001b); Beerling et al. (2002, 2009b); Greenwood et al. (2003); Royer (2003); Haworth et al. (2005); Passalia (2009); Retallack (2009); Quan et al. (2010); Smith et al. (2010)
CO_2-phytoplankton	Freeman and Hayes (1992)
CO_2-liverworts	Fletcher et al. (2008)
CO_2-nahcolite	Lowenstein and Demicco (2006)
Temp-tropical $\delta^{18}O$	Wilson and Opdyke (1996); Pearson et al. (2001, 2007); Wilson and Norris (2001); Norris et al. (2002); Wilson et al. (2002); Moriya et al. (2007); Pucéat et al. (2007); Bornemann et al. (2008)
Temp-tropical Mg/Ca	Tripati et al. (2003); Bice et al. (2006); Sexton et al. (2006)
Temp-tropical TEX_{86}	Schouten et al. (2003); Dumitrescu et al. (2006); Forster et al. (2007a,b); Pearson et al. (2007); Wagner et al. (2008)
Temp-benthic $\delta^{18}O$	Cramer et al. (2009)

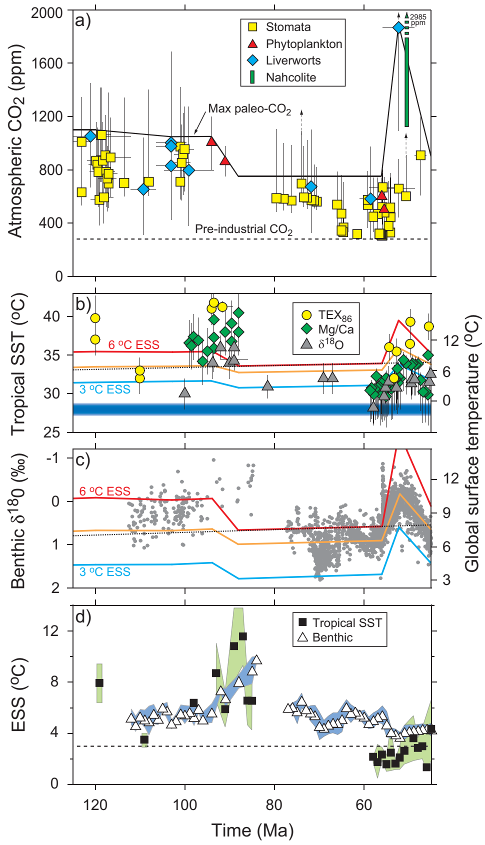

Fig. 1. See caption on next page.

Fig. 1. Atmospheric CO_2, temperature, and Earth system sensitivity (ESS) during the Cretaceous and early Paleogene. **(a)** Atmospheric CO_2 from multiple proxy approaches. Estimates with unbounded upper limits are noted with arrows. The nahcolite estimate has a flat probability (equal likelihood) between 1125 and 2985 ppm, but this range will likely be revised downward following new mineral equilibria experiments (Jagniecki et al., 2010). See Methods and Table 2 for data sources. **(b)** Tropical sea surface temperature (SST) and **(c)** benthic $\delta^{18}O$ records (see Table 2 for sources). Minimum global mean surface temperature is expressed relative to the pre-industrial (see Methods for details of calculation). The red and blue lines correspond to an ESS of 6 °C and 3 °C, respectively, as calculated from the "max paleo-CO_2" line in panel a and a pre-industrial baseline of 280 ppm. The orange lines represent an ESS of 6 °C up to the point of ice sheet decay (assumed to be triggered at 560 ppm CO_2, or one doubling; DeConto and Pollard, 2003; Pollard and DeConto, 2005; Royer, 2006; DeConto et al., 2008; Pearson et al., 2009), then 3 °C thereafter in an ice-free world. The dashed lines represent an ESS of 3 °C and a constant 2000 ppm CO_2. The blue band in panel **(b)** is the range of pre-industrial tropical SST (27–29 °C). **(d)** Calculation of ESS from the "max paleo-CO_2" line in panel a and temperature data in panels **(b)** and **(c)**, after correcting for changes in solar luminosity. Each data point is a 10 million year mean; errors are $\pm 1\sigma$. Time steps represented by one data point are not shown. Dashed line is an ESS reference of 3 °C.

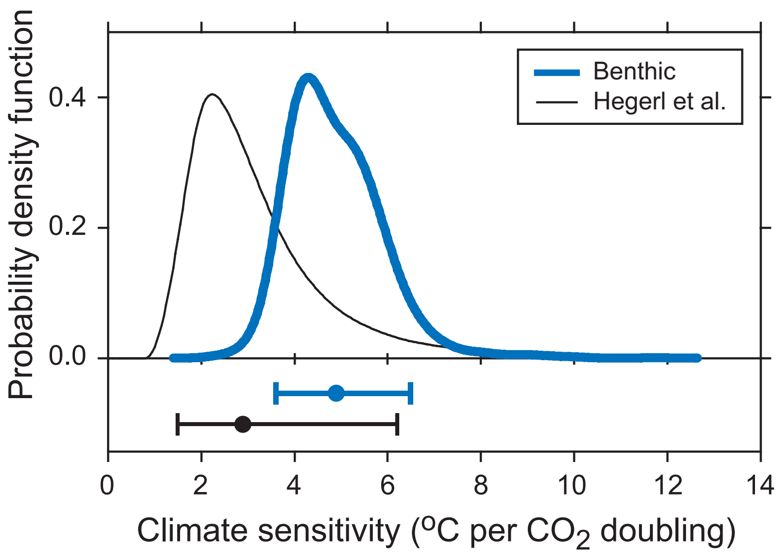

Fig. 2. Probability density function of the raw benthic data from Fig. 1d. Function was computed by kernel density estimation (Silverman, 1986). The Hegerl et al. (2006) function is a summary of Charney sensitivity based on historical records, proxy records over the last 1000 years, and model simulations. Circles and lines at bottom refer to means and 5–95% confidence limits.

Discussion Paper | Discussion Paper | Discussion Paper | Discussion Paper |